An Impedance Based Modeling Towards the Aging Prediction of Lithium-Ion Battery for EV Applications

Federico Martin Ibanez, Tanvir Ahmed and Ildar Idrisov
Energy Systems CREI
Skolkovo Institute of Science &Technology
Moscow, Russia
FM.Ibanez@skoltech.ru, Tanvir.Ahmed@skoltech.ru, I.Idrisov@skoltech.ru

Jose Sebastian Gutierrez
Facultad de Ingenieria
Universidad Panamericana
Aguascalientes, Mexico
jsgutierrez@up.edu.mx

***Abstract*— Modeling of Lithium-Ion Battery (LIB) is essential for studying its behavior under different operating conditions like temperature, load current and state of charge. The parameters of a LIB such as capacity, open circuit voltage, impedance can be characterized by using a suitable model according to the application. This paper has proposed an impedance-based equivalent circuit modeling (ECM) approach for electric vehicles (EV) to estimate the aging of a LIB ($LiFePO_4$) and to prevent the system, where the battery is installed, from failure. The aging has been performed experimentally using a real electric motorcycle load profile and the impedance test results for the aged LIB at different cycles have been fitted and analyzed with a chosen ECM. In addition, the same ECM has been used to analyze and compare the aging for the same battery type with a profile achieved using a hybrid energy storage system (HESS) consisting of LIB and supercapacitors. The ECM for HESS profile showed smaller impedance change and smaller capacity reduction with aging compared with the ECM for the battery profile. Therefore, it validates that HESS has a longer cycle life than battery energy storage system.**

Keywords— Aging, Cycle, Equivalent circuit model, Electric vehicles, Lithium-Ion battery, Hybrid energy storage system, Supercapacitor.

I. INTRODUCTION

Since the oil-gas driven traditional combustion-engine vehicles are one of the major reasons for air pollution and the greenhouse gas emissions, electrification of vehicles has become an important concern among researchers and manufacturers. For the last few decades, EV market such as micro and mild hybrid electric vehicle (HEV), plugged-in electric vehicle (PHEV) and battery electric vehicle (BEV) is increasing at a remarkable rate [1-4]. Thus, the demand for longer lifetime of energy storages calls for further development and understanding of the batteries in EVs.

Lithium-Ion batteries (LIB) are the most popular choice to be implemented in the EV applications due to their high energy density and reasonable lifetime. LIB can have a life cycle from 300 to 1500 cycles depending on different conditions such as temperature, depth of discharge, charge and discharge rate and aging [5].

LIB aging refers to the degradation phenomenon of its capacity and power capability with time due to physical and chemical changes inside the battery irrespectively of the condition whether it is being operated or not.

When the capacity and power capabilities decrease to a certain level, the service life of the LIB is over. Capacity fade refers to the loss in discharge capacity and power fade is the decrease of the power capability caused by an increase in the battery´s internal impedance [6].

LIB aging can occur in two ways: the calendar aging and the cycle aging. Calendar aging refers to the degradation of the charge capacity of battery during storage condition and cycle aging occurs when the battery goes through any charge-discharge cycle process. The last one is more complex to predict than calendar aging because it involves more independent variables such as depth of discharge, current profiles and temperature [7].

In this paper, an impedance model of LIB that includes the cycle aging effects for EV applications is presented. The model was extracted from measurements in a charge-discharge cycle test using a real power profile of an electric motorcycle.

Internal impedance and battery capacity have been measured periodically to observe the battery degradation through the cycles. From those measurements, an equivalent circuit model was obtained. The model parameters and the battery capacity change with the number of cycles. Thus, using this model, it is possible to roughly estimate the battery capacity based on the impedance measurements.

978-1-7281-3587-8/19/$31.00 ©2019 IEEE

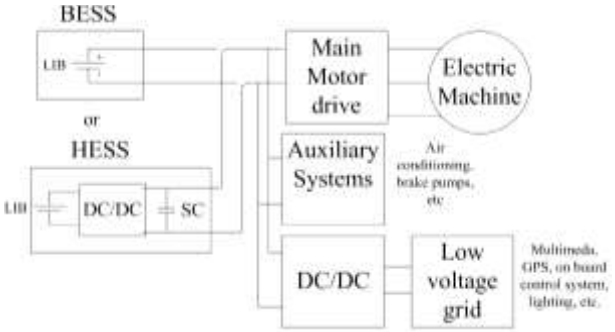

Fig. 1: EV main diagram with BESS or with HESS

Furthermore, the same model and the same cycle test was applied to a hybrid energy storage system (HESS) based on supercapacitors and lithium ion batteries and the battery was measured inside the HESS. Thus, this battery delivers a smoother current profile than in the first case (the only LIB-based energy storage system). Fig. 1 shows a typical block diagram of the power stage in an EV for the two scenarios: the battery-based energy storage system (BESS) and the HESS.

The results show different frequency range behaviors. The proposed model is focused in middle frequency range (0.1Hz – 1 kHz) due to the ease to measure in real time applications.

The paper is structured as follows: Section II reviews the Equivalent Circuit Modelling (ECM) for the aging of LIBs. Section III discusses the aging testing procedure through an EV load profile for a chosen LIB and Section IV analyzes the impedance test results and model parameters as a function of the number of cycles. Finally, Section V details the conclusion.

II. Battery Modeling

The battery modeling is useful to study its performance such as capacity, impedance under various operating conditions like temperature, load current, state of charge (SOC) and to identify when the battery is close to its end of life. This allows to predict lifetime for EV applications. Several battery models from different perspectives have been reported in the literature [8-14]. The choice of the model is a trade-off between model complexity, accuracy, and parameterization effort. The models found in the literature can be categorized into the following groups:

A. Empirical Modeling

These models use simple empirical equations to describe specific features of battery behavior. Such a simple model is the 'Peukert equation' based model [9], which is used to estimate the influence of current rates on the available capacity of a battery. The equation is:

$$C = I^k t, \quad (1)$$

where C is the capacity of the battery in Ah, I is the discharge current in A, k is Peukert's constant and t is the time in hours. The value of Peukert's constant varies depending on the type of batteries. For lead acid and nickel metal hydride batteries, the Peukert constant ranges between 1.08 and 1.15 with exception of Valve Regulated Lead Acid (VRLA) battery which shows high value of 1.28. While Lithium-ion batteries have k values between 1 and 1.09 [15], for example in [16] k=1.033 was obtained. The accuracy of empirical models is usually low for dynamic load conditions where the error can be as substantial as 100% [17] and only suitable in specific applications under constant current and constant temperature conditions.

B. Electrochemical Modeling

These models include reaction kinetics of the charge storage process as well as of relevant side-reactions, electric and mass transport in porous and electrodes, and thermal effects like self-heating. Such models are necessarily complex, usually expressed as a system of nonlinear partial differential equations and allow the analysis of the interdependencies of several effects. Despite higher complexity, they produce a high degree of accuracy [18].

C. Equivalent Circuit Modeling (ECM)

Equivalent circuit models (ECM) are generally used to describe the dynamic behavior of current and voltage at the terminals of a battery, regardless of the precise physicochemical processes within the cells. It consists of circuit elements such as resistors, capacitors, inductors and constant voltage source. They are widely used in various types of EV modeling simulations and offer a higher accuracy compared with empirical approaches [19-20]. ECM can be utilized to understand the batteries' behavior. In this paper, two ECM are discussed, one based on Voltage-Current (VI) and the other based on impedance spectroscopy methodologies.

1. VI based ECM

VI based ECMs are suitable for on-board measurements. A linear ECM structure can be used for this case consisting of voltage source representing the open circuit voltage which can be a function of state of charge (SOC) and temperature, a resistor representing for the internal resistance, and a few RC networks representing the dynamic behavior of the battery [21]. For example, the Thevenin model is illustrated in Fig.2. The model is governed by:

$$v_t = V_{OC} + R_0 i_L + v_{th}, \quad (2)$$

$$i_L = C_{th}\frac{dv_{th}}{dt} + \frac{v_{th}}{R_{th}}, \quad (3)$$

$$\dot{SOC} = \frac{i_L}{Q}, \quad (4)$$

$$V_{OC} = f(SOC). \quad (5)$$

Eq. (2) shows that for a given current i_L, the terminal voltage, v_t, is comprised of the open circuit voltage, V_{OC}, the voltage drop over the internal resistance $R_0 i_L$ and the drop over RC section v_{th}. v_{th} and SOC are governed by ordinary differential equations, given by (3) and (4) respectively.

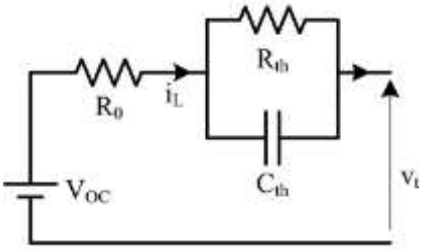

Fig. 2: Thevenin Equivalent Circuit Model of LIB

2. Impedance-based ECM

In this approach, battery impedance is measured by electrochemical impedance spectroscopy (EIS). The ECM's parameters of an ECM can be identified by fitting the model to the measured battery's EIS. Usually, nonlinear parameter identification methods are required for this. Common ECM used for this purpose is Randle's equivalent circuit shown in Fig.3 [22]. It consists of a double layer capacitance C_l in parallel to a reaction resistance R_1 which is in series with a resistance R_0 that represents the ohmic resistance of the electrolyte and inductance that represents the battery's inductive behavior in the high-frequency region.

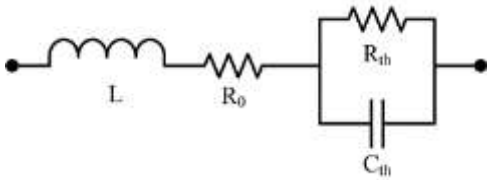

Fig. 3: Simplified Randle's Equivalent Circuit

The total impedance Z for the model can be written as

$$Z = Z_L + Z_{R_0} + Z_{R_1 \| C_1}, \quad (6)$$

where Z_L is the impedance due to the inductance observed in the high-frequency region, Z_{R_0} is the ohmic resistance of the battery and $Z_{R_1 \| C_1}$ is the impedance of the battery during the charge transfer phenomena. Eq. (6) can be rewritten as:

$$Z = j\omega L + R_0 + \frac{R_1 \times \frac{1}{j\omega C_1}}{R_1 + \frac{1}{j\omega C_1}} = j\omega L + R_0 + \frac{R_1}{1 + j\omega R_1 C_1} \quad (7)$$

In this paper, this model is chosen, but the inductance has not been considered because most of the applications operate in the low to the mid frequency range. So, the impedance becomes,

$$Z = R_0 + \frac{R_1}{1 + j\omega R_1 C_1} \quad . \quad (8)$$

For obtaining the model using EIS, the battery was tested with an impedance meter. The result, which shows the impedance (real and imaginary parts) from 1000 KHz down to 10 mHz, are commonly presented on a Nyquist plot. This information is the input for the fitting process to obtain the model. In the model parametrization presented in this paper, this method was used during the cycling process to observe the parameter change due to the cycling aging.

III. LIB AGING TESTING PROCEDURE

A 50Ah, 3.2V LIB ($LiFePO_4$) has been chosen for the aging purpose. Fig. 4.a shows the test bench that has been developed for cycling the LIB. The test bench has a DC programmable power supply which is used for charging the battery with constant voltage constant current (CC-CV) charging method. An electric scooter's current load profile was applied to the LIB as the load profile using a programmable load. An acquisition unit was used for acquiring the voltage and the current of the LIB and a software in Matlab-Simulink platform was used for controlling the test bench. Fig. 4.b presents the main diagram of the test bench, where the main components can be identified. In the following paragraphs the cycle procedure is detailed.

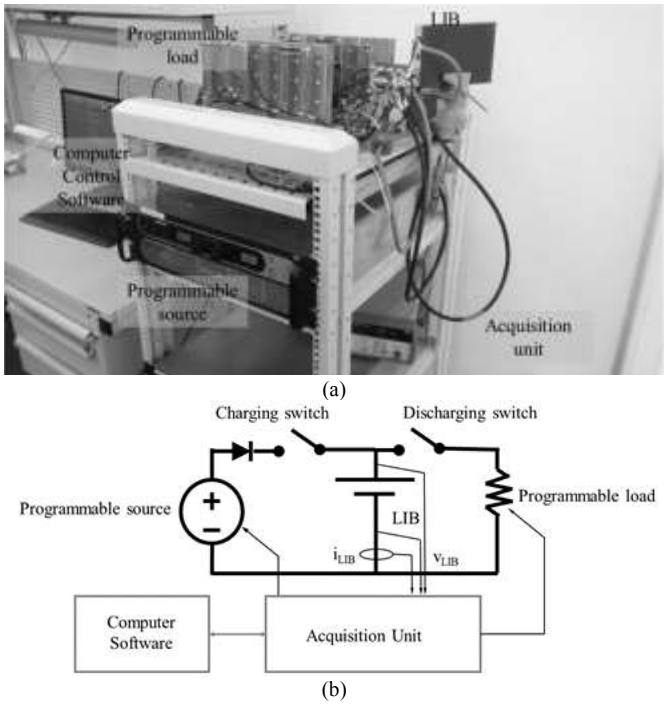

Fig. 4: Battery cycling test bench: (a) prototype, (b) block diagram

The LIB is charged up to the maximum cutoff voltage (3.7V) using the DC programmable power supply through the CC-CV method at 50A (1C). After the charging is finished, the system is switched to the discharging mode and the LIB starts to discharge using the programmable load following the current load profile of electric scooter.

Fig. 5.a shows the discharge profile of a real electric motorcycle which consists of a branch of 22 LIBs like the one that was tested in this research, therefore the voltage is close to 70V instead of 3.2V. The main characteristics of the motorcycle are: in-wheel 5kW brushless motor, weight of 200 kg, a battery of 70V 50Ah and a motor drive which can work in the range from 60V to 100V [16].

In this paper, two discharge profiles were analysed. The first one, is the discharge profile that was obtained directly from the motorcycle using only a battery based storage system. The second profile was obtained considering that the storage system is an hybrid energy storage system (HESS) based on the the same battery with the aid of supercapacitors. Fig. 5.b shows the profile of the battery inside the and the block diagram of the different components of the motorcycle with the HESS.

For the cycle procedure, the current discharge profile was mimicked because each cell has the same current in a series branch. The discharge process continuously repeats the discharge profile until the LIB reaches the cut-off discharge voltage (set as 2.5V). Thus, one full cycle is completed, a typical cycle is shown in Fig 6. This charge and discharge process is repeated during more than 250 cycles. The cycle takes two hours approximately.

The current and voltage profiles for a full cycle (including charge and discharge is shown in Fig. 6.a and b). Positive current means discharging current and negative current means charging current. In the charging mode, it is observable that the charging current did not exceed 50A. This is due to the fact that the maximum charging current suggested by the manufacturer is 50A or 1C rate. The maximum charging cut-off voltage was set to 3.7V and the minimum discharge cut-off voltage to 2.5V according to the battery datasheet.

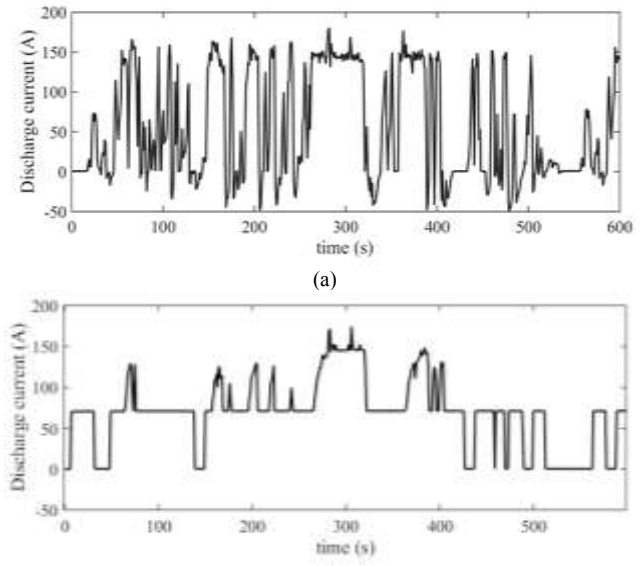

Fig. 5: (a) battery discharge profile collected from a real electric motorcycle including the motorcycle block diagram, and (b) battery profile using a HESS

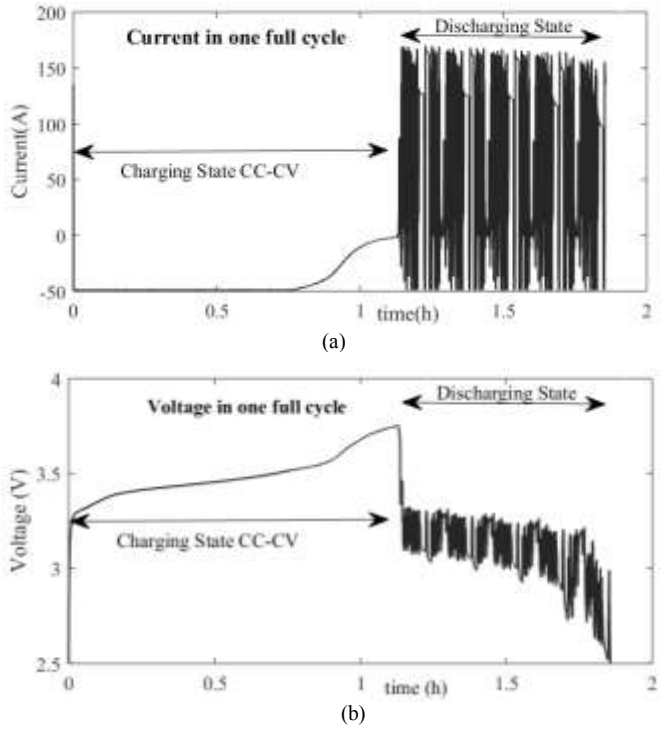

Fig. 6: LIB (a) current and (b) voltage for one cycle

IV. Model Fitting with Impedance Plot

Two parameters which are the impedance (in mΩ) and the capacity (Ah) of the LIB were measured through the whole cycling experiment to analyze the aging of device under test.

A. Impedance Measurement

The impedance spectrum had been observed in the frequency range of 100kHz-10mHz through Nyquist plot by using EC-lab potentiostat software platform. 350 cycles have been conducted for the tested LIB. Before each impedance measurement, the cycling was stopped and then the battery was kept in no-load condition during one hour to stabilize the electric charge. Fig. 7 shows the results at different number of cycles. Three effects can be observed.

The first is that at high frequencies, all of the curves present series inductive-resistive behavior, from there the series resistance of the Randle's cell can be easily extracted as the real part of the impedance (see Fig. 7). The second effect is the semi-circle, which represents the RC tank in the Randle's cell, there, as the number of cycles increases the frequency at the semi-circle middle point decreases. This indicates an increment in the cut-off frequency of the RC tank, in other words an increment in the tank resistance or capacitance. The third effect is the 45° slope at the end of every curve. This is effect is due to the diffusion process in the battery and it cannot be modelled with the simple Randle's cell and the frequency is low enough for real-time measurements (mHz range). Finally, it can be mentioned that at high frequencies, an inductance effect is appreciated, what it means that the curves go down vertically at high frequencies.

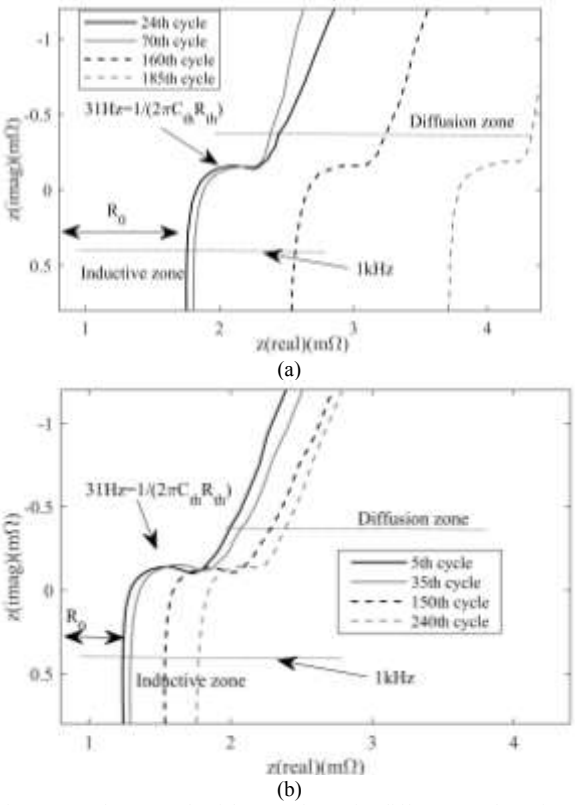

Fig. 7: Impedance result of the tested LIB for different number of cycles in (a) BESS and in (b) HESS

B. Model Fitting with Impedance plot

The plots achieved from the EIS test for the different number of cycles were then fitted with the simplified ECM discussed in section II (Randle's cell). As most of the applications operates in low to mid frequency range, the range for extracting the model was limited from 2Hz to 1 kHz. Thus, the inductance and the diffusion behaviors were neglected. In this fitting, as frequency tank $(2\pi C_{th}R_{th})^{-1}$ practically does not change, the main parameter was R_0. Fig. 8 shows the results for both cases, the BESS and the HESS.

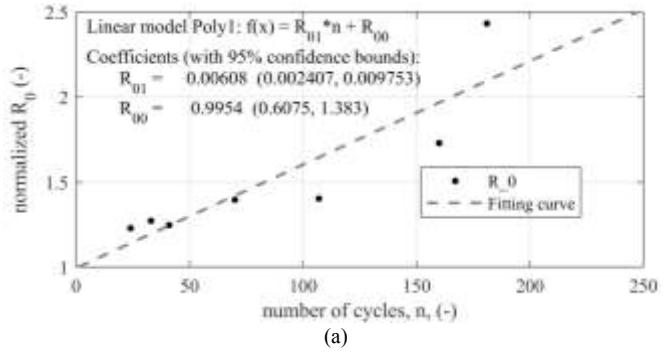

(a)

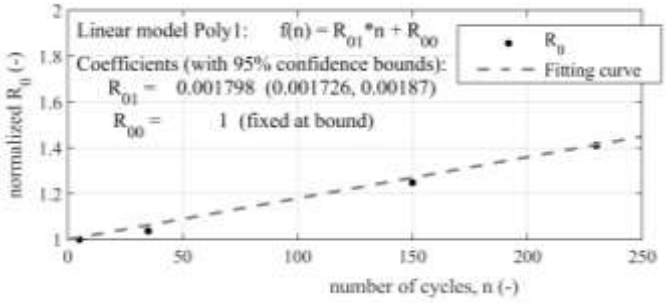

(b)

Fig. 8: Fitted Curve for R_0 for (a) BESS and (b) HESS

The values for R_0 show a linear increasing trend. A simple first-degree polynomial equation was used to predict the impedance behavior as a function of the number of. The R-square index that measures the goodness of fitting of the curve with equation, were computed and is 0.95 in the HESS case and 0.82 in BESS case. Although the accuracy is not high, with this simple equation, Fig. 8 shows clearly the increase in R_0 as the number of cycles increases. Therefore, it is possible to estimate the number of cycles of a LIB by measuring those circuit parameters. The obtained equation that relate the number of cycles (n) with R_0 is:

$$R_0 = R_{01}.\ n + R_{00}, \tag{9}$$

where R_{01} and R_{00} are the coefficients of the first degree linear fitting. The BESS has around three times higher impedance than the HESS.

C. Capacity Measurement

The capacity of the two storage systems (BESS and HESS) has been calculated from the measured current values and is illustrated in Fig. 9. Notice, that the capacity in HESS is much less reduced compared to BESS for the same number of cycles. This trend can also be understood based on the R_0 trend, the capacity reduction is about three times lower in HESS then in BESS. Using the same technique, it is possible to estimate LIB capacity as a function of the number of cycles with a linear trend as:

$$C_{Ah} = C_{Ah1}\ .\ n + C_{Ah0}, \tag{10}$$

where C_{Ah1} is the slope, and C_{Ah0} is the initial capacity value. Therefore, using the same technique, it is possible to estimate LIB capacity as a function of the number of cycles with a linear trend as:

$$\Delta C_{Ah} = C - C_{Ah0} = \frac{C_{Ah1}}{R_{01}}(R_0 - R_{00}) = \frac{C_{Ah1}}{R_{01}}\Delta R_0 \tag{11}$$

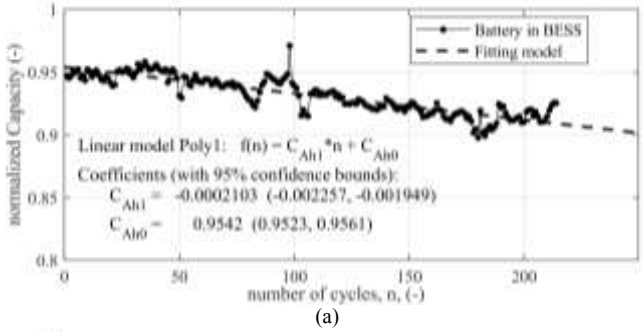

(a)

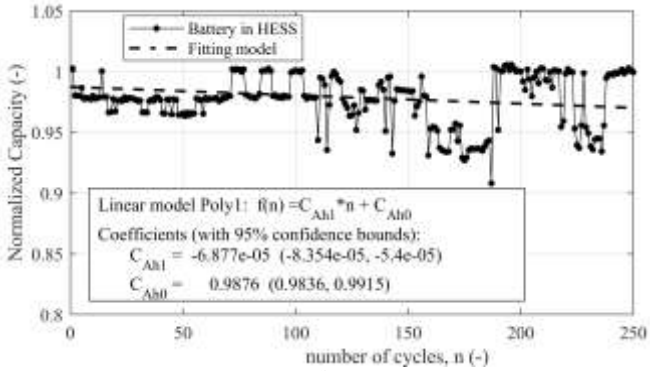

(b)

Fig. 9: Battery capacity degradation with increased number of cycles (a) in BESS and (b) in HESS

CONCLUSION

The paper shows a simple equivalent circuit model which was used to predict roughly the capacity of the battery based in the impedance measurement. It shows the connection between the battery resistance and capacity (Ah), so based the capacity reduction can be estimated as a function of the battery resistance.

In order to validate the benefits of the model, two types of storage systems were analyzed experimentally: BESS and HESS. The model shows that the increase in the HESS impedance as a function of the number of cycles is three times lower than the BESS. Furthermore, a reduction in the battery capacity in BESS is also three times higher than in HESS, which validates the model. Therefore, the relation between impedance increase and capacity reduction is a tool for estimating the remaining cycle life.

REFERENCES

[1] G. A. Putrus, P. Suwanapingkarl, D. Johnston, E. C. Bentley, and M. Narayana, "Impact of electric vehicles on power distribution networks."

IEEE Vehicle Power and Propulsion Conference, pp. 827-831, Dearborn, Oct. 2009.

[2] M. Thele, J. Schiffer, E. Karden, E. Surewaard, D.U. Sauer, "Modeling of the charge acceptance of lead–acid batteries", Journal of Power Sources, vol. 168, no. 1, pp. 31-39, 2007.

[3] O. Topal, "Electric bus concept against to diesel and CNG bus for public transport operations.", 5th International Istanbul Smart Grid and Cities Congress and Fair (ICSG), pp. 105-109, Istanbul, 2017.

[4] A. Elgammal, and A.M. Sharaf, "A hybrid pv-fc-diesel-battery efficient schemes for four-wheel PMDC electric vehicle drive system", International Journal of Renewable Energy Research (IJRER), vol. 2, no. 1, pp. 53-77, 2012.

[5] M. Ecker, N. Nerea, K. Stefan, S. Johannes, B. Holger, A. Warnecke and D.U. Sauer, "Calendar and cycle life study of Li (NiMnCo) O2-based 18650 lithium-ion batteries", Journal of Power Sources, vol. 248, pp. 839-851, 2014.

[6] K. Uddin, P. Surak, W. Widanage, L. Somerville, and J. Marco, "Characterising lithium-ion battery degradation through the identification and tracking of electrochemical battery model parameters." Batteries, vol. 2, no. 2, 13, 2016

[7] S.F. Schuster, T. Bach, E. Fleder, J. Müller, M. Brand, G. Sextl and A. Jossen, "Nonlinear aging characteristics of lithium-ion cells under different operational conditions." Journal of Energy Storage, vol. 1 pp. 44-53, 2015.

[8] J. Jiang, and C. Zhang, "Fundamentals and applications of Lithium-Ion batteries in electric drive vehicles" John Wiley & Sons, 2015.

[9] P. Kurzweil, "Gaston Planté and his invention of the lead-acid battery—The genesis of the first practical rechargeable battery" in Journal of Power Sources, vol. 195, no. 14, pp. 4424-4434, 2010.

[10] G. Gwak and H. Ju, "Thermal Modeling of Lithium-ion Batteries with LiFePO4 Electrodes," 2018 7th International Conference on Renewable Energy Research and Applications (ICRERA), Paris, pp. 824-830, 2018.

[11] Yao-Ching Hsieh, Tin-Da Lin and Ruei-Ji Chen, "Li-ion battery model exploring by intermittent discharging," 2012 International Conference on Renewable Energy Research and Applications (ICRERA), Nagasaki, pp. 1-5, 2012.

[12] N. Somakettarin and T. Funaki, "An experimental study on modeling of transient response and parameters identification for Mn-type Li-Ion battery with temperature dependency," 2014 International Conference on Renewable Energy Research and Application (ICRERA), Milwaukee, WI, pp. 804-809, 2014

[13] J. Badeda, M. Huck, D. U. Sauer, J. Kabzinski, and J. Wirth, "Basics of lead-acid battery modeling and simulation." In Lead-Acid Batteries for Future Automobiles, pp. 463-507. 2017.

[14] V.H. Johnson, "Battery performance models in ADVISOR", Journal of Power Sources, 110(8),321–329,2002.

[15] N. Omar, M. Daowd, P.V. Bossche, O. Hegazy, J. Smekens, T. Coosemans, and J.V. Mierlo, "Rechargeable energy storage systems for plug-in hybrid electric vehicles—Assessment of electrical characteristics." Energies 5, no. 8, pp 2952-2988, 2012

[16] F.M. Ibanez, A.M.B. Florez, S. Gutiérrez and J.M. Echeverrría, "Extending the Autonomy of a Battery for Electric Motorcycles," in IEEE Transactions on Vehicular Technology, vol. 68, no. 4, pp. 3294-3305, April 2019.

[17] A. Hausmann, and C. Depcik, "Expanding the Peukert equation for battery capacity modeling through inclusion of a temperature dependency." Journal of Power Sources, vol. 235, pp. 148-158, 2013

[18] R. Klein, N.A. Chaturvedi, J. Christensen, J. Ahmed, R. Findeisen, and A. Kojic. "Electrochemical model based observer design for a lithium-ion battery." ,IEEE Transactions on Control Systems Technology, vol 21, no 2, pp. 289-301, 2012.

[19] L. Zhang, Z. Wang, X. Hu, F. Sun and D.G. Dorrell, " A comparative study of equivalent circuit models of ultracapacitors for electric vehicles." Journal of Power Sources, 274, pp. 899-906, 2015.

[20] H. He, R. Xiong and J. Fan, " Evaluation of lithium-ion battery equivalent circuit models for state of charge estimation by an experimental approach." energies, *4*(4), pp. 582-598, 2011.

[21] F.M. Ibañez, J.M. Echeverria, J. Vadillo, F. Martin, L. Fontan, "Battery Response Analyzer using a high current DC-DC converter as an electronic load", International Conference on Renewable Energy and Power Quality (ICREPQ'11), pp. 13-15, 2011.

[22] Randles, J.E. Brough, "Kinetics of rapid electrode reactions." Discussions of the faraday society, vol. 1, pp. 11-19, 1947